Available online at www.sciencedirect.com
SCIENCE DIRECT®
Journal of Catalysis 225 (2004) 190–202
JOURNAL OF CATALYSIS
www.elsevier.com/locate/jcat

A fundamental study of Pt tetraammine impregnation of silica 1. The electrostatic nature of platinum adsorption

Marc Schreier and John R. Regalbuto *

Department of Chemical Engineering, University of Illinois at Chicago, 810 South Clinton, Chicago, IL 60607, USA

Received 28 January 2004; revised 19 March 2004; accepted 24 March 2004

Available online 12 May 2004

Abstract

The adsorption of $Pt(NH_3)_4^{+2}$ onto five different amorphous silicas (fumed and precipitated) was studied as a function of pH and concentration of platinum in solution. The ability of silica to protonate and deprotonate as a function of pH leads to an electrostatic attraction of the +2 platinum cation in the basic pH range, where the silica surface is negatively charged. Adjusting for the differences in surface area of the various silicas, and since all have about the same point of zero charge (PZC), the adsorption behavior is similar for all materials. Platinum uptake as functions of pH and metal concentration is reasonably simulated by the revised physical adsorption (RPA) model using the same set of independently measured parameters for all five silicas. This is the same model that has been previously employed to describe the adsorption of anionic Pt chloride complexes over alumina in the acidic pH range [Chem. Eng. Sci. 56 (2002) 3491]. The proton balance included in the model also accounts for shifts in pH, which are virtually the same with and without metal in solution. Because of this, and because the maximum extent of Pt adsorption appears to have a steric limit and is much less than that predicted by an "ion-exchange" mechanism, we believe that "electrostatic adsorption" is a more precise description of the adsorption mechanism. In a second paper among other issues we show that platinum complexes adsorbed onto silica at the optimal pH of about 10 remain 100% dispersed after reduction.

Keywords: Silica; Physical adsorption; Ion exchange; Platinum tetraammine; Catalyst impregnation

1. Introduction

Among the simplest, least expensive, and most prevalent preparation methods in the manufacture of heterogeneous catalysts is the process of impregnation, whereby high surface area porous supports such as silica and alumina are contacted with aqueous solutions containing dissolved metal complexes. After impregnation, wet slurries are dried to remove water and heated in various oxidizing and reducing steps to remove the metal ligands and to reduce the metal to its catalytically active state.

Much recent progress in the "transformation of the art of catalyst preparation into a science" has been made in catalyst impregnation through fundamental studies of the adsorption process. A landmark work is the postulation of Brunelle that the adsorption of noble metal complexes onto common oxides supports was essentially coulombic in nature [2]. The hydroxyl groups which populate oxide surfaces become protonated and so positively charged or deprotonated and negatively charged below a characteristic pH value [2,3]. This pH, at which the surface is neutral, is termed the point of zero charge (PZC). This surface hydroxyl chemistry is depicted in Fig. 1. Brunelle cited many instances in which oxides placed in solutions at pH values below their PZC would adsorb anions such as hexachloroplatinate $[PtCl_6]^{-2}$, while at pH values above their PZC would adsorb cations such as platinum tetraammine (PTA), $[(NH_3)_4Pt]^{+2}$. This electrostatic mechanism was semiquantitatively developed by another landmark work, that of Contescu and Vass [4], who studied the adsorption of $[PdCl_4]^{-2}$ and $[(NH_3)_4Pd]^{+2}$ over alumina at low and high pH, respectively, and was soon followed by the comprehensive series of Heise and Schwarz for anionic Pt chloride adsorption over positively charged alumina at low pH [5–8].

Even while the electrostatic aspects of metal complex adsorption have been recognized in Brunelle's and other works on Pt ammine adsorption onto silica [2,9–13], the actual interaction of the Pt ammine complex with the silica surface is

* Corresponding author.
E-mail address: jrr@uic.edu (J.R. Regalbuto).

0021-9517/$ – see front matter
doi:10.1016/j.jcat.2004.03.034

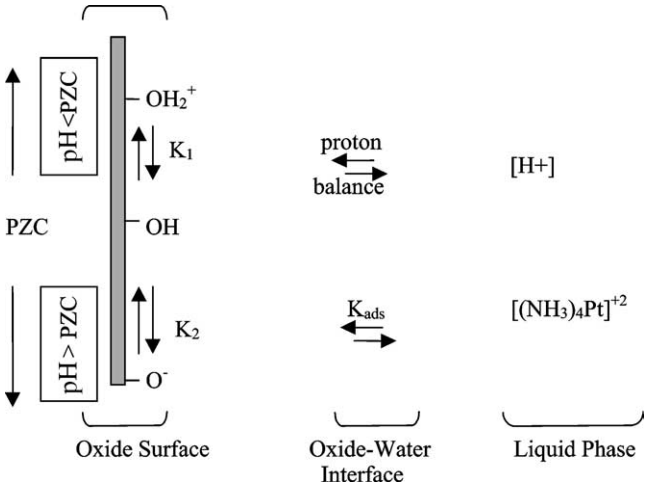

Fig. 1. Three regimes of the PTA/silica adsorption system.

most often described as "ion exchange," written in general [13] as

$$2(\text{Si–O}^-, \text{H}^+) + \left[\text{Pt(NH}_4)_3\right]^{+2}, (\text{OH}^-)_2 \longleftrightarrow (\text{Si–O}^-)_2, \left[\text{Pt(NH}_4)_3\right]^{+2} + 2(\text{H}^+, \text{OH}^-).$$

Our own work has dealt with the experimental verification and quantification of an electrostatic adsorption mechanism, building on the quantitative model first proposed by Healy and James [14]. Major components of the revised physical adsorption (RPA) model are a non-Nernstian treatment of the surface charge and potential, and a proton balance between the bulk liquid and the surface so that dramatic pH shifts occurring when aqueous solutions are brought into contact with oxides surfaces can be predicted [15]. This proton transfer is depicted in Fig. 1. Our first work with adsorption dealt mainly with simulations of cation adsorption over silica using a more rigorously derived (and much smaller) solvation energy term together with the non-Nernstian potential [16]. In later works we discovered that the solvation energy term can be omitted altogether [1,17]. The adsorption equilibrium constant (Fig. 1) can be calculated simply from the coulombic energy of interaction. With the RPA model, all known sets of chloroplatinic acid (H_2PtCl_6 or CPA)/alumina adsorption data can be satisfactorily simulated with no adjustable parameters [1,18].

In this paper, we wish to present a complementary system to CPA/alumina. That is, instead of analyzing the adsorption of an anionic complex, $[PtCl_6]^{-2}$, over a positively charged surface (alumina at low pH), we have measured and simulated the uptake of cationic Pt complexes ($[(NH_3)_4Pt]^{+2}$) over a negatively charged surface (silica at high pH). Both the reasonable agreement of the RPA model to the data and a number of experiments directed toward discriminating between the various mechanisms, namely ion exchange, suggest that the adsorption mechanism is again purely electrostatic in nature. A correlation between strong electrostatic adsorption and high metal dispersion in the reduced state is demonstrated in the following paper.

Table 1
Properties of silicas employed

Supplier	Name	Type	Surface area (m^2/gm)	PZC
Cabosil	L90	Fumed	90	4.3
Cabosil	M-7d	Fumed	200	4.2
Cabosil	EH-5	Fumed	380	4.2
Degussa	Vn-3s	Precipitated	175	4.1
Degussa	Fk-300	Precipitated	300	4.1

2. Experimental

The types of silica employed and their pertinent characteristics are shown in Table 1. Both fumed and precipitated silicas with varying surface areas were chosen. For ease of handling, the silicas were densified by wetting with deionized water and then drying at 373 K. The precipitated silicas contained significant sodium sulfate impurities, which were manifested by as-received PZC values near 6. These samples were washed with a solution of 0.001 M HNO_3, shaken for approximately 1 h, filtered, rinsed copiously with deionized water, dried overnight at 373 K, and calcined at 773 K for 3 h. The PZCs of the washed precipitated and the fumed materials were all found to be in the range 4.1–4.3. Illustrative data are shown later in the results.

Tetraammonium platinum chloride (99.9%) (or platinum tetraammine) was obtained from Aldrich and dissolved in solutions of various pH at concentrations of 78–2420 ppm. Platinum concentrations were measured by ICP (Perkin Elmer Optima 2000) before and after contact with silica to determine the Pt uptake. Control experiments in the absence of silica showed that the PTA complex was soluble over the pH range 2–13.5. Readings at the highest pH were slightly affected by the presence of Na^+ in solution. Typical reproducibility of Pt concentrations was ±5% at pHs below 11, and ±10% from 11 to 13.5. The ICP instrument was also used to estimate the Na concentration, which was complicated due to a complex matrix effect and a wide range of Na levels at the higher pH experiments. The accuracy of ICP measurements was improved by using a multiwavelength calibration, yttrium as an internal standard, multiple replicate data, and radial analysis mode. Dilutions of the original solutions were also run to confirm accuracy. The typical reproducibility was ∼ 95% in the pH range 1–10.5, and ∼ 90% at higher pH values. For Na, the reproducibility was ∼ 95% in the pH range 9–11.5, and ∼ 85% at higher pH.

Experiments were conducted in 60 ml polypropylene bottles containing 50 ml of solution and various amounts of silica. The mass of the silica was adjusted to account for the different surface areas, to give identical "surface loadings" or m^2 oxide per liter of solution. Surface loadings of 2000 m^2/L (great excess of solution, wet impregnation) and 30,000 m^2/L (near pore filling) were employed. The surface density, Γ_{Pt}, is calculated at the concentration of Pt adsorbed

divided by the surface loading, that is,

$$\Gamma_{\mathrm{Pt}} = \frac{(C_{\mathrm{Pt,init}} - C_{\mathrm{Pt,final}})\ (\mathrm{mole/L})}{\mathrm{SL}\ (\mathrm{m^2/L})} = \mathrm{uptake}\ (\mathrm{mole/m^2}).$$

Two main types of adsorption experiments were performed: uptake versus pH at constant metal concentration, and uptake versus metal concentration at constant pH. Silica-free control experiments were conducted in parallel with each adsorption run. After the solutions were pipetted into bottles containing the silica, the suspensions were placed on an orbital shaker and 5-mL portions were withdrawn at various time intervals and filtered (Biohit 22 μm) for ICP analysis. Measurements of pH were also made at this time. Kinetic runs were made to determine that 90% of Pt uptake over the well-mixed powders occurred within several minutes; contact times of 1 h were chosen for adsorption. Uptakes showed little difference (less than 5%) between 1 and 24 h; the 1 h contact time was assumed sufficient for the equilibrium.

Select samples from adsorption experiments were filtered off, calcined at different temperatures, and further reduced in H_2. The final catalysts were characterized and dispersion data was obtained.

3. Theory

The simplified RPA model used to simulate the data has been published previously [1,17]; a summary of the model has been appended. Model parameters are given in Table 2. A hydroxyl density of 5 OH/nm^2 has been taken from the literature [3,19,20]. The PZC and surface charging parameters K_1 and K_2 are measured independently of adsorption by obtaining best fits of pH shifts to Pt-free control experiments [19]. This fitting procedure will be shown under Results. The model employs a Langmuir isotherm in which the adsorption constant is calculated from the coulombic interaction between the charged complex and the potential at the plane of adsorption. Representative plots of surface charge and Pt uptake for PTA cation adsorption over silica are given in Fig. 2a. At the PZC the surface is not charged and no adsorption occurs. As the pH is raised above the PZC,

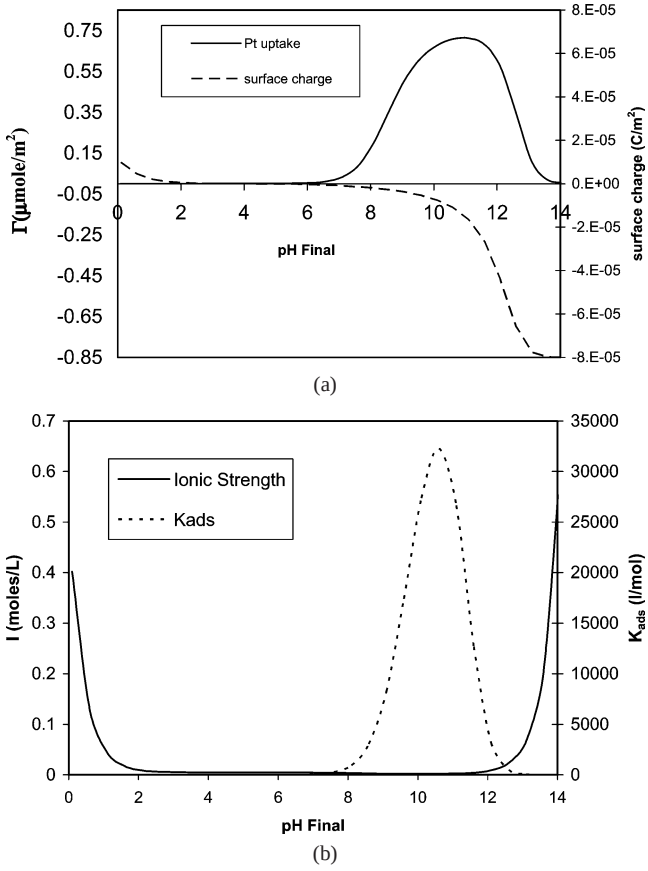

Fig. 2. RPA model for PTA/silica using the parameters of Table 2. (a) PTA uptake and surface charge versus pH, (b) ionic strength and adsorption equilibrium constant versus pH.

the surface charge (σ_0, C/m^2) increases and the uptake increases. The maximum extent of adsorption, Γ_{max}, for the cationic Pt ammine complex has been suggested by previous data [20] to be a close-packed layer of Pt complexes which retain two hydration sheaths. Based on the radius of PTA of 2.41 Å, and two diameters of water 2.76 Å, this maximum density is calculated to be 0.86 μmol/m^2, or about 1 complex per 2 nm^2. The anionic chloro complexes appear to retain only one hydration sheath [1,18,20], so maximum extent of adsorption is inherently higher by a factor of two for the anionic complexes. At high pH, adsorption is retarded

Table 2
Parameters used for RPA model of PTA/silica

Parameter	Symbols	Units	Range of values
Initial Pt concentration	$C_{\mathrm{Pt,Initial}}$	M (mol/L)	0.0004–0.012
Surface loading	SL	m^2/L	1000–30,000
Temperature	T	K	298.15
Initial pH	$\mathrm{pH_{int}}$	–	1.0–13.5
Radius of complex	r_i	Å	2.41
Valence	z	–	+2
No. of hydration sheaths	nhs	–	2
Point of zero charge	PZC	–	4.25
Surface acidity constant	$\mathrm{p}K_2 - \mathrm{p}K_1 = \Delta \mathrm{p}K$	–	7.25
Hydroxyl density	N_{s}	OH/nm^2	5.0

not by competition from Na^+, as many "chemical" models presume, but by the effect of high ionic strength, which effectively diminishes the value of the adsorption equilibrium constant [1,18]. The ionic strength and the adsorption equilibrium constant are plotted in Fig. 2b to illustrate this effect.

4. Results

4.1. Control experiments

In Fig. 3a, pH final is plotted versus pH initial for metal-free acid and base solutions contacted with silica at 30,000 m^2/L. The data appear similar for 2000 m^2/L, except that the pH plateau is narrower owing to the lesser amount of oxide in solution. The low surface loading data appear in a later figure in comparison with the pH shifts from Pt-containing solutions. The pH shift model, with PZC and ΔpK optimized for a best fit of both sets of data [19], is the solid black line; all five silicas were reasonably simulated with a ΔpK of 7.25 and a PZC of 4.25. From these control experiments it is seen that even at low surface loadings, the protonation–deprotonation chemistry of the hydroxyl groups at the silica surface causes significant shifts in solution pH.

Silica dissolution is plotted as a function of the final pH in Fig. 3b. Significant dissolution of the silica occurs above a pH of 10, in line with other works [2,3,21].

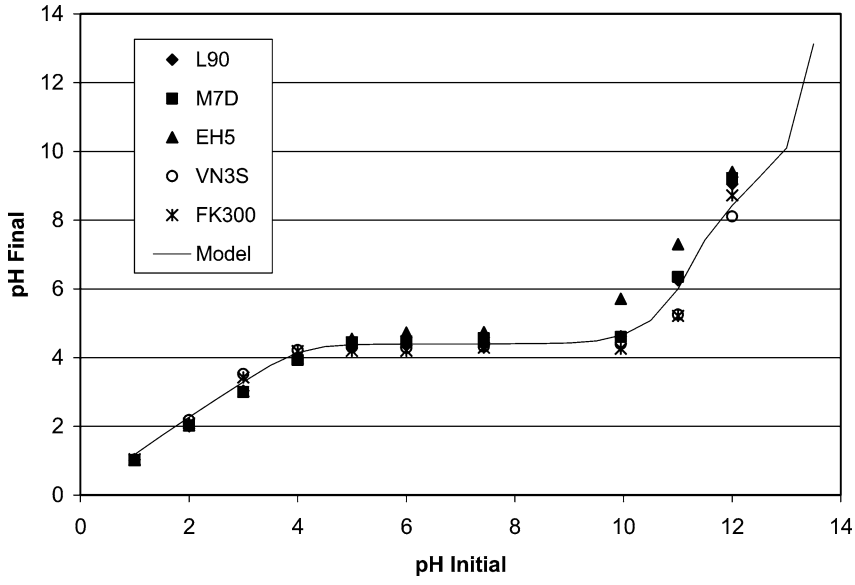

(a)

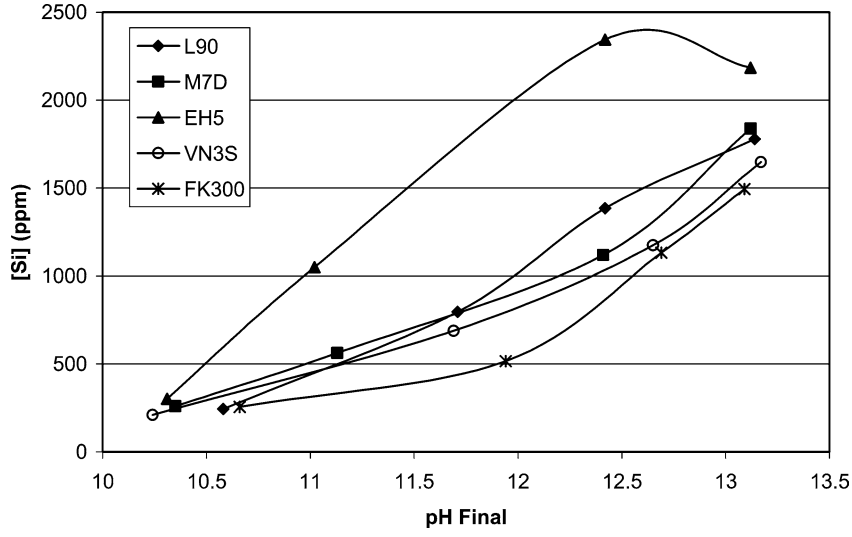

(b)

Fig. 3. Control experiments in Pt-free solutions, (a) pH shift data for Pt-free solutions contacted with silica at 30,000 m^2/L (best model fit obtained using PZC = 4.25, $\Delta pK = 7.25$), (b) silicon dissolution from various silicas versus pH, at 2000 m^2/L.

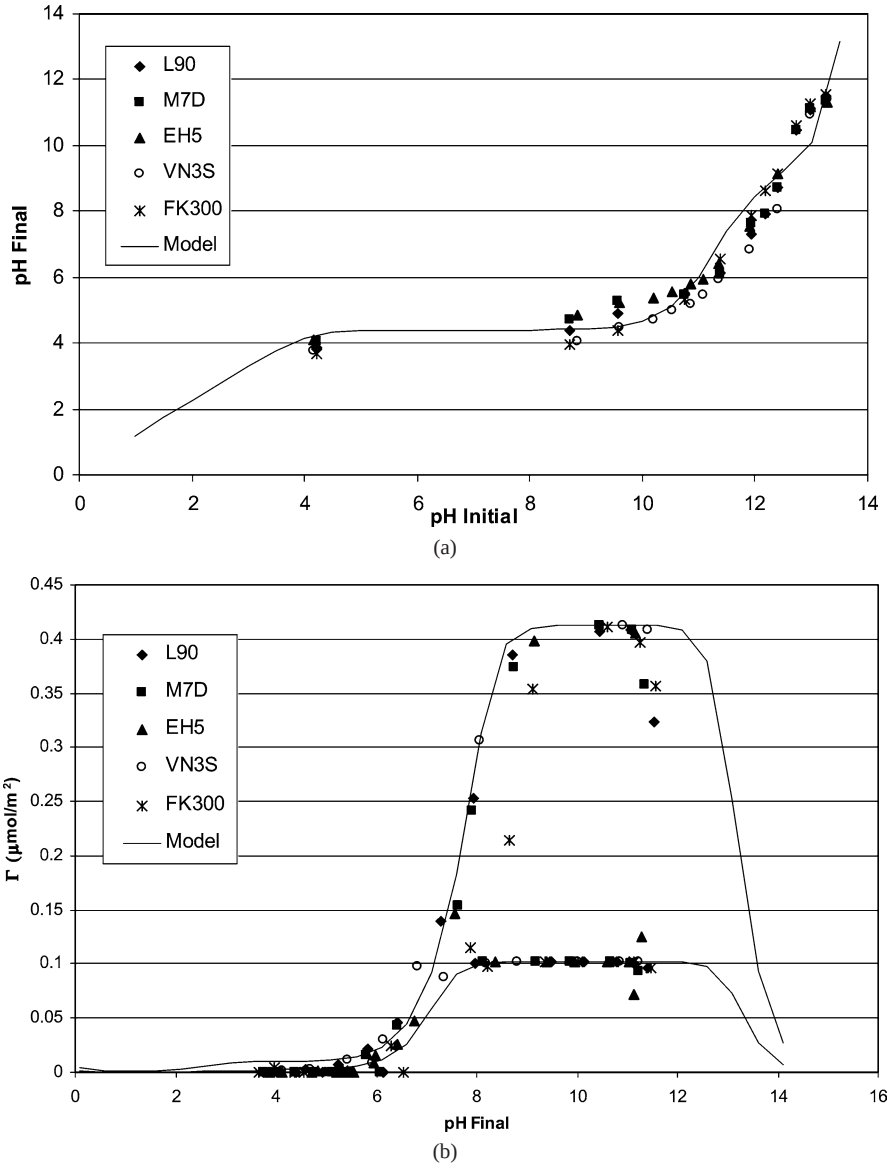

Fig. 4. PTA uptake versus pH at high surface loading (30,000 m^2/L). Modeled using PZC = 4.25, $\Delta pK = 7.25$.

4.2. Adsorption surveys

Adsorption surveys were performed at initial pH values in the range of 2–13.5. The results of contacting 2420 and 600 ppm Pt with 30,000 m^2/L silica are shown in Fig. 4; the shifts in pH are given in Fig. 4a (for the 2420 ppm Pt solutions), and the uptake of Pt is shown in Fig. 4a. In both figures the RPA model, using the parameters obtained from the control runs, is represented as a solid black line and fits the data well. Significant uptake begins only past an equilibrium pH of 6, and then reaches a wider or narrower plateau, at the low and higher concentration, respectively, as both concentrations are below the monolayer adsorption capacity (they correspond to 1/8 and 1/2 of a monolayer). The decrease in uptake as pH becomes very high is consistent with the RPA model effect of high ionic strength, which diminishes the adsorption equilibrium constant.

In Fig. 5, various results are shown from an uptake experiment at 2000 m^2/L. The pH shifts are similar to Fig. 4a and are not shown. Platinum uptake vs final pH is given in Fig. 5a for two concentrations, 312 and 78 ppm, which correspond to a full and $\frac{1}{4}$ monolayer. At the lower concentration a pronounced plateau is once again observed. The uptake curve shows the sharpest maximum at a pH of about 10.5–11 for the higher concentration experiment, since this is the highest concentration relative to the surface loading. The RPA model, using the same set of parameters as for all other figures, gives a reasonable fit to the adsorption data as well as the pH shift data (not shown).

Additional data for silica dissolution, Na uptake, and 24-h adsorption were collected for the 2000 m^2/L experiment.

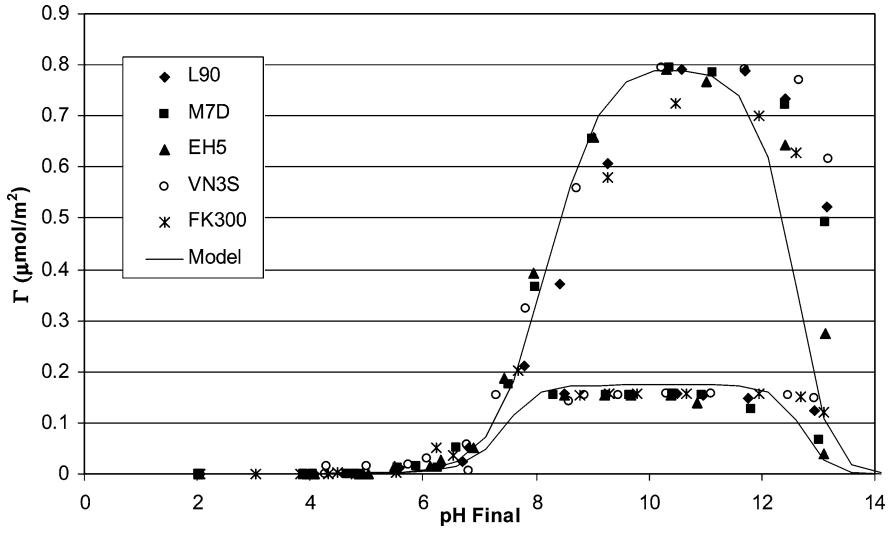

(a)

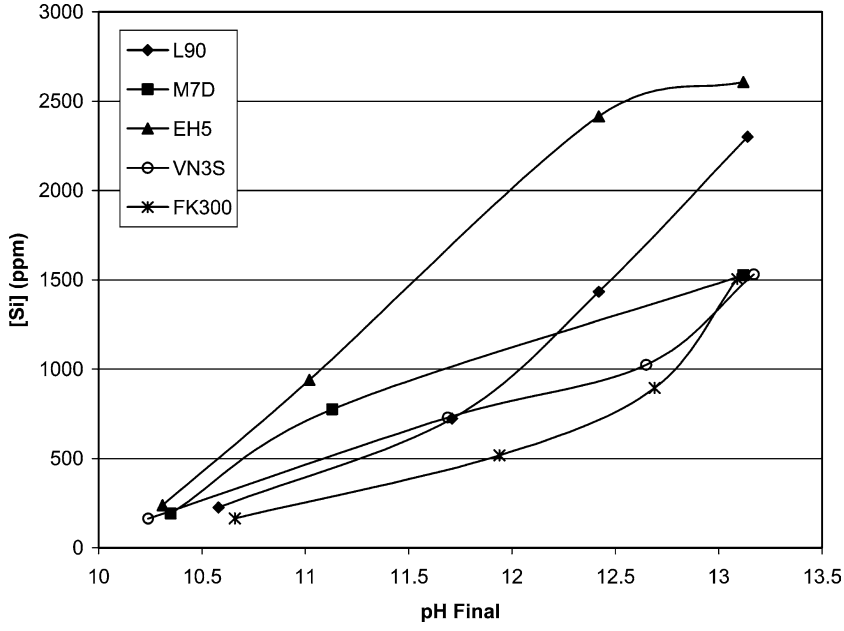

(b)

Fig. 5. PTA adsorption experiment at low surface loading (2000 m^2/L). (a) PTA uptake versus pH, (b) dissolved silicon versus pH, (c) Na uptake versus pH, and (d) uptake after 24 h (312 ppm). Modeled using PZC = 4.25, $\Delta pK = 7.25$.

Silica dissolution vs pH final data is shown in Fig. 5b; significant dissolution of silica occurs above a final pH of 10.5. In Fig. 5c, Na uptake is plotted vs pH final data in the region of significant Pt adsorption. These data indicate that generally little or no Na is adsorbed in the high pH range. Vn-3s (precipitated silica) may exhibit some uptake of Na at pH values of 11.7 and 12.6; yet there is still close to a monolayer of Pt adsorbed. This conflicting set of data may simply arise from ICP scatter in the Na data. Fig. 5d shows Pt adsorption vs pH final (24 h) data with the RPA model represented as a solid black line. The uptake curve is almost identical to the uptake curve after 1 h (Fig. 5a, 312 ppm). The decrease in Pt uptake at long contact time at the high pHs is thought to be due to a loss of silica surface due to extensive dissolution.

Other adsorption experiments were performed keeping the final pH constant (~ 10.5, maximum uptake) and varying the initial concentration of Pt in solution. Figs. 6a and 6b show Pt adsorption (Γ_{Pt}) vs initial Pt (ppm) in solution data for 1000 and 5000 m^2/L with the RPA model represented by a solid black line. As the initial concentration of Pt in solution increases the uptake of Pt plateaus around 0.7–0.9 μmol/m^2 and then decreases slowly as the initial concentration of Pt is increased. The slow decrease in surface density at higher Pt concentrations is once again consistent with the RPA model effect of high ionic

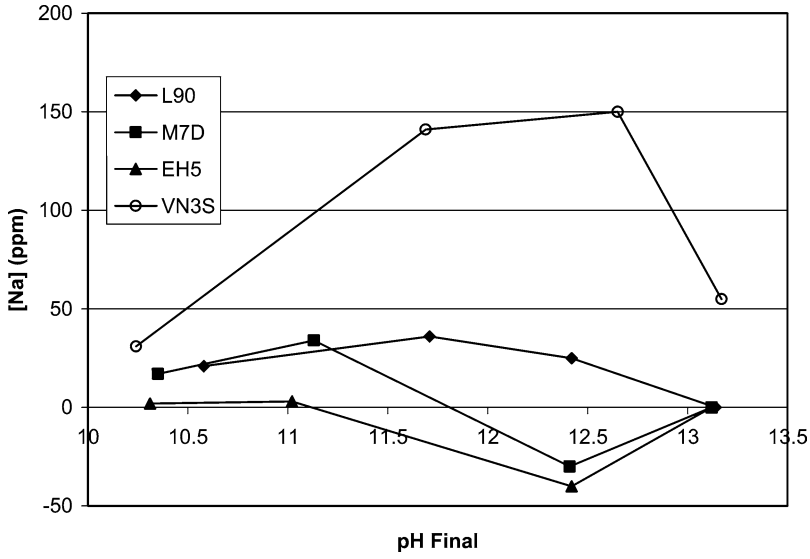

(c)

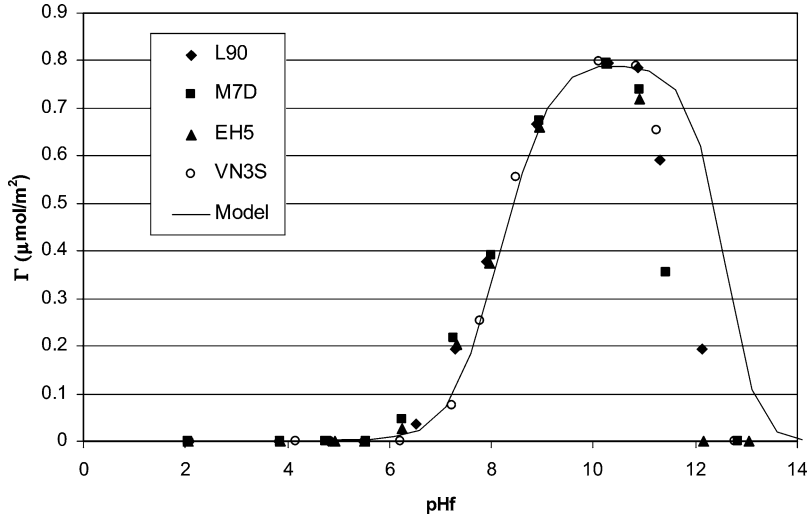

(d)

Fig. 5. (Continued.)

strength (Fig. 2); once the silica surface is saturated, the additional PTA remains in solution, increasing the ionic strength.

4.3. Washing experiments

To test the effect of washing on the reversibility of adsorption, an additional adsorption experiment was performed at 2000 m^2/L, employing an initial amount of Pt in solution equal to one monolayer of coverage. The initial pH of 12.5 was chosen for optimal adsorption (∼ 100%) at a final pH of 10.5. The slurry was shaken for 1 h. The ICP analysis confirmed that ∼ 100% of the Pt was adsorbed. The solution was filtered off and 3 g of the solid was added to 50 mL of DI water (a great excess of solution) at pH 5.8. The final pH of the mixture, however, was approximately 10.11. ICP analysis of the mixture showed negligible Pt loss. This is to say that washing of the sample did not cause a loss of Pt, because the pH was still very high and so the Pt complexes were still strongly adsorbed. Next, 0.1 M HCl was added dropwise to a pH of 4.0. This solution was shaken for approximately a half hour. The pH of the final solution was 4.37 and ICP analysis confirmed 211 ppm (∼ 95–100% originally adsorbed) of Pt in solution.

5. Discussion

5.1. Ion exchange vs electrostatic adsorption

As a first topic of discussion we would like to distinguish between the adsorption mechanisms of “ion exchange” and “electrostatic adsorption.” The ion-exchange reaction noted in the Introduction has been used from the earliest through

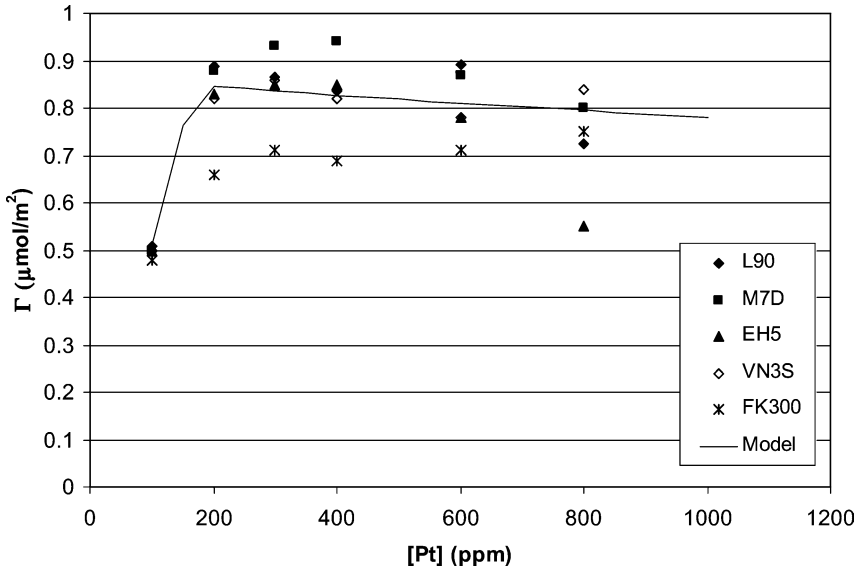

(a)

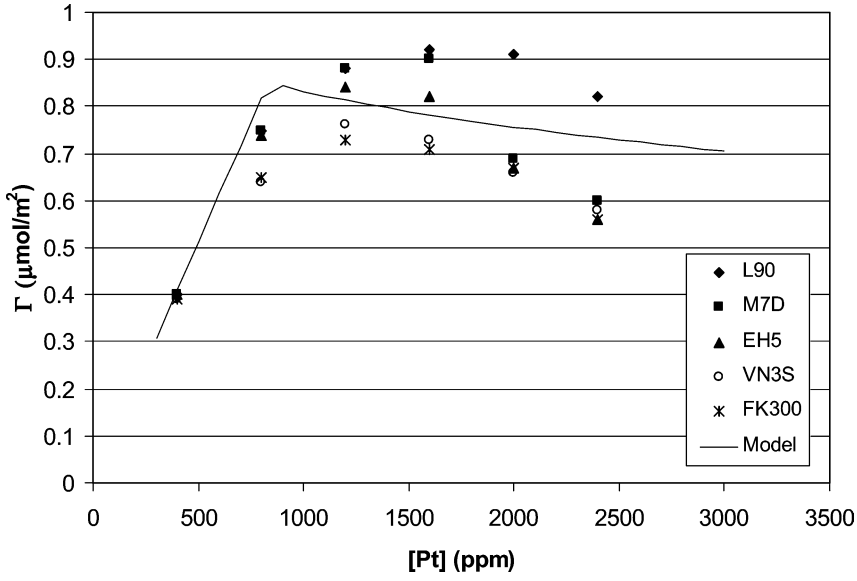

(b)

Fig. 6. Platinum uptake at final pH 10.5 versus PTA concentration for (a) 1000 m^2/L and (b) 5000 m^2/L. Modeled using PZC = 4.25, $\Delta pK = 7.25$.

the latest [2,9–13] works to represent the deposition of Pt ammines onto silica. When the chloride and not the hydroxide salt is used (as in the present study) the ion-exchange reaction becomes

$$2(\text{Si–O}^-, \text{H}^+) + \left[\text{Pt(NH}_4)_3\right]^{+2}, (\text{Cl}^-)_2 \longleftrightarrow (\text{Si–O}^-)_2, \left[\text{Pt(NH}_4)_3\right]^{+2} + 2(\text{H}^+, \text{Cl}^-).$$

Written as such, several mechanistic aspects are implied. First, Pt complexes can interact over a neutrally charged surface and produce protons, and second, Pt ammines deposit over the hydroxyl groups at the silica surface in a 1:2 stoichiometry. Careful inspection of the literature and the present data call these mechanistic features into question.

Considering the first issue, the independence of Pt adsorption and proton release is clouded by the proton transfer that occurs to and from the surface OH groups in response to the bulk pH, in the absence of an adsorbing metal. The dramatic buffering effect oxides have on acid and base solutions has been thoroughly demonstrated [22] and quantitatively modeled [15]. When placed into solutions at pH values above its PZC of about 4, hydroxyl groups at the silica surface deprotonate and the solution becomes more acidic. The changes in pH in the presence and the absence of adsorbing Pt complexes can be made by comparing the pH shift data from the control experiment (such as in Fig. 3) and the adsorption experiment (such as in Figs. 4 and 5). This comparison is shown in Fig. 7 for representative samples at the

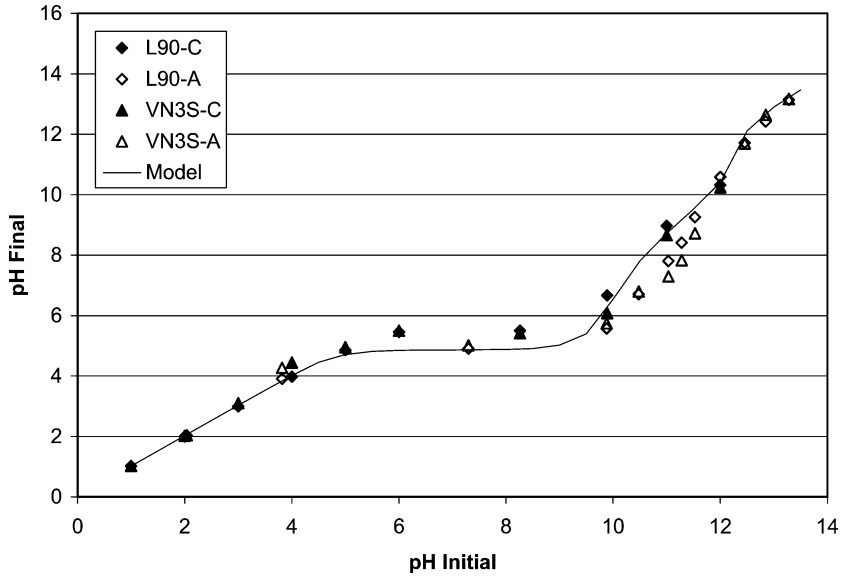

(a)

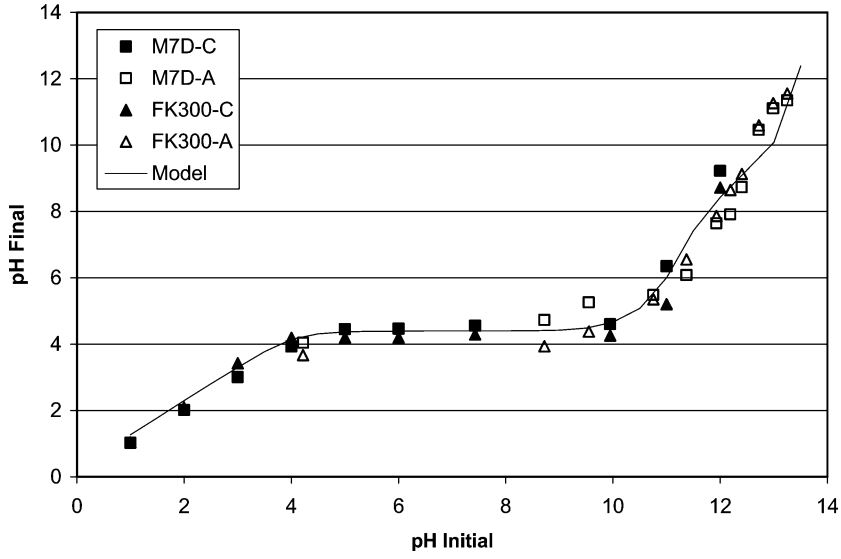

(b)

Fig. 7. Comparison of pH shifts for Pt-free and Pt-containing solutions over representative silicas at (a) 2000 m^2/L (with 312 ppm Pt solutions), (b) 30,000 m^2/L (with 2420 ppm Pt solutions). Modeled using PZC = 4.25, $\Delta pK = 7.25$.

lower surface loading (Fig. 7a) and the higher surface loading (Fig. 7b). Shifts of the higher Pt concentrations were used, but pH shifts for the lower Pt concentrations were essentially the same. The data in both plots very nearly overlap over the whole pH range. The greatest discrepancy is seen at the control run final pH of 9 (both plots), where the final pH of the Pt-containing sample is a little less than 8. This corresponds to a difference in the OH^- concentration of about 10^{-5} M. From Fig. 4b it is seen that at a final pH of 9, approximately 2400 ppm of Pt has been adsorbed. This corresponds to a Pt concentration of over 10^{-2} M, or at least 1000 times in excess of the discrepancy in final pH values. Considered another way, if the proton released/Pt adsorbed ratio is taken as 2, the protons released by adsorption, beyond the normal proton exchange in Pt-free conditions, would bring the final pH down to around 2.9. This does not occur; we interpret the similarity of pH changes in Pt-free and Pt-containing solutions to mean that proton transfer and Pt adsorption are independent phenomenon. The simulated uptake and pH shifts were calculated on this basis, and show good agreement to the pH shift data of both the control and the adsorption runs (Figs. 3 and 4), and the uptake data of the latter (Figs. 4 and 5).

A second argument against an ion-exchange mechanism can be made by comparing the amount of Pt adsorbed to the OH site density. Cited hydroxyl densities of amorphous silica surfaces in liquid solutions are typically around 5 OH/nm^2 [3,21,23]. The maximum uptake we observe,

over five different sets of silicas at a wide range of surface loading (Fig. 6) is near 0.86 μmol/m^2, or 0.5 complex/nm^2, which is an order of magnitude less than the OH density. The highest Pt loading reported by Benesi et al. [9] over a 370 m^2/g silica was 0.30 mmol, corresponding to about 0.56 complex/nm^2. The surface density of the highest Pt loading reported by Brunelle [2], 5.5 wt% over a 260 m^2/g silica, is also about 0.6 complex/nm^2. In Goguet et al. [13], about 0.4 mmol of Pt are adsorbed over a 194 m^2/g silica, giving about 1.1 complex/nm^2. While this loading is about twice that of the others, it is still far below the OH site density.

Thus it appears that the Pt-adsorbed/OH site density is much less that 1:2. In the RPA model the maximum surface density of Pt ammines corresponds to a steric monolayer of Pt ammine complexes (radius = 2.41 Å) which retain 2 hydration sheaths (2.78 Å). Thus the area per complex is about $\pi^*[2.41 + (2)(2.78)]^2$ Å^2 = 2.0 nm^2. In earlier work we have noted that chloride complexes of Pt appear to adsorb with one hydration sheath intact, leading to a maximum density of about 1 complex/nm^2 [1,18]. The maximum Pt loading which can be obtained by strong electrostatic adsorption is then directly proportional to the silica surface area, and is inherently a factor of two lower than can be achieved using the chloride complex over an appropriate support (i.e., one with a neutral to basic PZC such as alumina that can accrue a strong positive charge).

A final indication that ion exchange is not occurring is the absence of a correlation in the dissolved Na concentration, seen in Fig. 5c, with Pt uptake, Fig. 5a. Assuming one Na can adsorb for each deprotonated OH, and a density of 5 OH/nm^2, silica with 200 m^2/g at 2000 m^2/L has the capacity to adsorb 400 ppm of Na. The uptake of Na is generally much lower than this. Furthermore, above pH 11 where Pt uptake falls off, there is no concomitant increase in Na concentration.

In sum, we believe that the mechanism of adsorption of PTA over silica at high pH is much more accurately described as electrostatic adsorption than it is ion exchange. Instead of Pt ammines exchanging in precise ratios at specific OH groups on the silica surface, we envision the independent processes of the accrual of a negative surface charge at high pH, followed by the coulombic attraction of the cationic complexes, which at the optimal pH, reach a monolayer of close-packed complexes retaining two hydration sheaths. At the highest pH values, uptake decreases due to high ionic strength and an effective decrease of the adsorption equilibrium constant. We would suggest that ion exchange is more appropriately applied to systems such as cationic exchange in zeolites in which the exchange reaction occurs at a particular site (the Brönsted acid site) and in a stoichiometric amount determined by the aluminum content. We have found cationic exchange of Pt ammines to be pH independent over a variety of zeolites [24].

Sermon and Sivalingam [25] have taken a more complex chemical approach to the PTA/silica system. In addition to ion exchange they suggest that silica dissolution acts like a "chemical glue." It has been well documented that silica dissolves in the basic region [2,3,21]. Following Fig. 5b, silica dissolution indeed increases in the high pH range. However in Fig. 5a, platinum adsorption decreases in the same range (10.5–13) as silica dissolution increases. This is opposite of the behavior to be expected were silica a chemical glue. Furthermore, in Figs. 8a and 8b, silica dissolution vs pH final data for both adsorption and control experiments is compared. The amount of dissolved silica is the same in both the presence and the absence of Pt. We take this to mean that silica dissolution is independent of adsorption. At long contact times (Fig. 5d), silica can dissolve to such an extent that a significant fraction of the surface is lost and the uptake of PTA decreases. Since silica dissolution is a kinetic phenomenon, it is not taken into account by the RPA model. The retardation of PTA adsorption over silica at high pH, even at short contact times (Fig. 5a) is analogous to the retardation of CPA at low pH over alumina [1,18], and is explained (see Fig. 2b) by the diminishment of the adsorption equilibrium constant at high ionic strength.

5.2. *Practical implications: a strong electrostatic adsorption—high final dispersion correlation*

Brunelle expressed the hope that the initial high dispersion of adsorbed Pt complexes could be retained through the reduction step, and indeed he reported particles sizes of 10 to 20 Å produced from Pt ammine precursors adsorbed onto silica at high pH [2]. Likewise, Benesi et al. prepared catalysts at or near 100% dispersion using a combination of Pt ammine salts (by a relatively complex "ion-exchange" formulation) which resulted in the deposition of Pt ammines at high pH [9]. Adsorbing Pt ammines at pH 9 with and without ammonia, Goguet et al. produced particle sizes in the 15–20 Å range (about 65–50% dispersed, respectively) [13]. From our adsorption results, it can be surmised that the optimal pH range for strong electrostatic adsorption is about 10.5 (Fig. 5), at which point Si dissolution is minimal. This is also the point at which essentially all Pt is adsorbed from solution; that is, even though an excess of solution might be utilized for the preparation, no Pt would be wasted were the supernatant solution to be decanted. As reported under Results, there appears to be little concern that Pt ammines will desorb during washing once they are strongly adsorbed. In the following paper we present a comprehensive study of the effect of preparation method and pretreatment condition on Pt dispersion [26]. We demonstrate that a simple wet impregnation in which Pt ammines (from any salt) are adsorbed at the optimal pH can yield small reduced particles which are 100% dispersed.

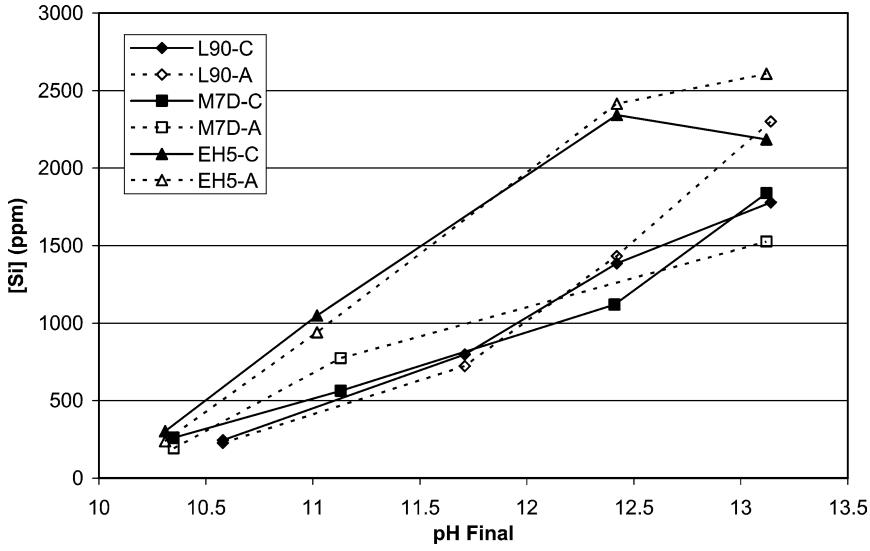

(a)

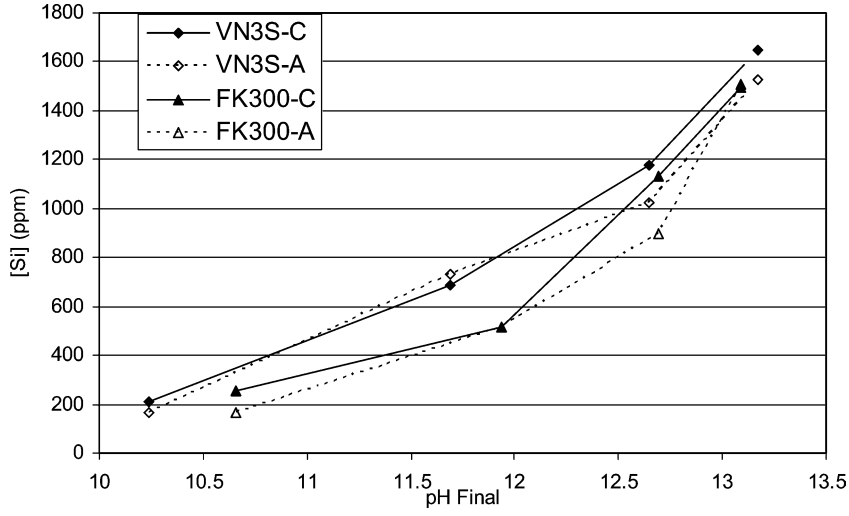

(b)

Fig. 8. Comparison of silica dissolution in Pt-free and Pt-containing solutions (*xx* ppm), at 2000 m^2/L, (a) fumed silicas, and (b) precipitated silicas.

6. Conclusions

At least for short contact times, it appears that PTA adsorption over silica at high pH obeys essentially the same electrostatic mechanism as anionic chloroplatinate adsorption over alumina at low pH. The systems show analogous pH dependence; increasing uptake as the pH moves away from the PZC, and then retardation at the pH extreme due to high ionic strength. In both systems, support dissolution and proton transfer appears to be independent of adsorption. Because adsorption appears to occur only after the surface has charged, and because the maximum extent of adsorption appears to be governed by a steric limit and not by stoichiometry, we believe the process to be more accurately considered as electrostatic adsorption than ion exchange. On a practical note, Pt complexes deposited onto the silica surface at the optimal pH, that is, in the regime of "strong electrostatic adsorption" can yield reduced metal particles with 100% dispersion.

Acknowledgment

The support of the National Science Foundation (CTS 99-08181) is gratefully acknowledged.

Appendix A

A.1. Surface model: pH shift [15] with CO_2 adsorption

The surface site balance [Eq. (A.1)] describing the surface charge (σ_0) by the difference of positively charged protonated sites (MOH_2^+) and negatively charged deprotonated

sites (MO^-) divided by the total number of sites is

$$\frac{\sigma_0}{F\Gamma_t} = \frac{[MOH_2^+] - [MO^-]}{[MOH_2^+] + [MOH] + [MO^-]}, \tag{A.1}$$

where F is the Faraday constant and Γ_t is the density of charged sites in moles/m^2. The charging mechanism is described by the following two equations:

$$[MOH_2^+] \overset{K_1}{=} [MOH] + [H_s^+], \tag{A.2}$$

$$[MOH] \overset{K_2}{=} [MO^-] + [H_s^+]. \tag{A.3}$$

Assuming the law of mass action, the intrinsic acidity constants can be written

$$K_1 = \frac{[MOH][H_s^+]}{[MOH_2^+]}, \tag{A.4}$$

$$K_2 = \frac{[MO^-][H_s^+]}{[MOH]}, \tag{A.5}$$

where $[H_s^+]$ is the proton concentration at the oxide surface. A Boltzman distribution relates the surface to the bulk proton concentration

$$[H_s^+] = [H^+]\exp(-y_0). \tag{A.6}$$

Rearranging Eqs. (A.4), (A.5), and (A.6) and substituting into Eq. (A.1), the site balance equation becomes

$$\frac{\sigma_0}{F\Gamma_t} = \frac{\{[H]^+\exp(-y_0)/K_1\} - \{K_2\exp(y_0)/[H]^+\}}{\{[H]^+\exp(-y_0)/K_1\} + 1 + \{K_2\exp(y_0)/[H]^+\}}. \tag{A.7}$$

The intrinsic acidity constants are defined as

$$K_1 = 10^{(-PZC+0.5\Delta pK)}, \tag{A.8}$$

$$K_2 = 10^{(-PZC-0.5\Delta pK)} \tag{A.9}$$

and y_0 is defined as follows, where e is the charge of an electron, k is the Boltzman constant, T is temperature in Kelvin, and ψ_0 is the surface potential:

$$y_0 = \frac{e\psi_0}{2kT}. \tag{A.10}$$

The Gouy–Chapman equation describing the relationship between the surface charge and the potential is

$$\sigma_0 = (8\varepsilon\varepsilon_0 kTn_0)^{1/2}\big[\exp\big((ze\psi_0)/(2kT)\big) - \exp\big(-\big((ze\psi_0)/(2kT)\big)\big)\big]. \tag{A.11}$$

The third equation is a proton balance of the liquid phase.

$$\sigma_0 = (F/SL)\big[\big\{[H^+]_0 - [OH^-]_0\big\} + \big\{10^{-(14-pH)} - 10^{-pH}\big\}\big](c^0/\gamma), \tag{A.12}$$

where the activity coefficient (γ) is described using the extended Debeye–Huckel equation and I is the ionic strength.

$$\gamma = 10^{-0.510(\sqrt{I}/(1+\sqrt{I}))}, \tag{A.13}$$

$$I = 10^{-pH} + 10^{(pH-14)} + \sqrt{0.01x_{CO_2}C_{tot,CO_2}K_{H_2CO_3}}, \tag{A.14}$$

where the mole fraction of CO_2 is found from the vapor liquid equilibrium and is a function of the ionic strength of the solution.

$$f_{vap,CO_2} = x_{CO_2}P_{sat}\gamma. \tag{A.15}$$

Equations (A.7), (A.11), (A.12), and (A.15) are solved using a Newton–Raphson method for the surface charge, potential, mole fraction of CO_2, and the equilibrium (final) pH at initial pH values.

A.2. Adsorption equations; revised physical adsorption (RPA) model [16,17]

The RPA model assumes a Langmuir isotherm to describe the physical adsorption of anions or cations onto oxide surfaces.

$$\Gamma_t\left(\frac{\text{mole}}{\text{area}}\right) = \frac{\Gamma_{max}K_iC_i}{1 + K_iC_i}, \tag{A.16}$$

where Γ_{max} is the maximum adsorption density based on a steric close-packed layer of the adsorbates retaining one or two hydration sheaths.

$$\Gamma_{max} = \left[\frac{1}{N_0\pi(r_i + 2nhs\,r_w)^2}\right]. \tag{A.17}$$

N_0 is Avogadro's number, r_i is the radius of species i, r_w is the radius of water, and nhs is the number of hydration sheaths retained. Generally speaking cations tend to retain two hydration sheaths and anions tend to retain one. The adsorption equilibrium constants for species i are described by

$$K_i = \exp\left(\frac{-\Delta G_{ads,i}}{RT}\right), \tag{A.18}$$

where the Gibbs free energy of adsorption in the simplified RPA model is simply set equal to a coulombic Gibbs free energy term described as

$$\Delta G_{ads,i} = \Delta G_{coul,i} = z_iF\Psi_{x,i}, \tag{A.19}$$

where z_i is the charge of species i, F is the Faraday constant, and $\Psi_{x,i}$ is the potential of species i at some distance x found by a Laplace solution of Gouy and Chapman assumpting a simple electric double layer is

$$\Psi_{x,i} = \left[\frac{2RT}{ZF}\right]\ln\left[\frac{(Y+1) + (Y-1)e^{-\kappa x_i}}{(Y+1) - (Y-1)e^{-\kappa x_i}}\right], \tag{A.20}$$

where x_i and Y are

$$x_i = r_i + 2nhs\,r_w, \tag{A.21}$$

$$Y = \exp\left(\frac{ZF\Psi_0}{2RT}\right). \tag{A.22}$$

κ is the Debey–Huckel reciprocal double layer length and is a function of the ionic strength.

$$\kappa = 3.31 \times 10^9\sqrt{I}, \tag{A.23}$$

$$I = 0.5\sum_i z_i^2C_i. \tag{A.24}$$

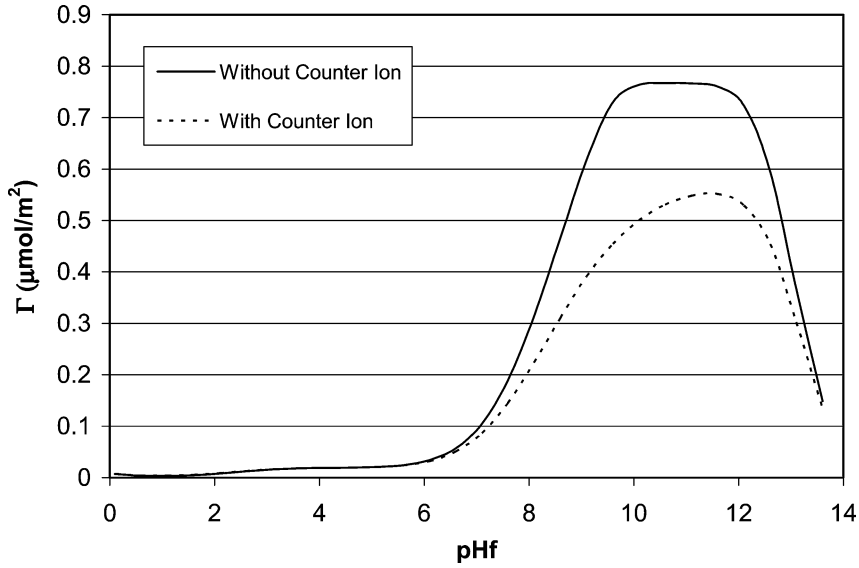

Fig. A1. Comparison of counterion effect in the simplified RPA model. Solid line with out counterion, dashed line with counterion. Modeled using PZC = 4.25, $\Delta pK = 7.25$, surface loading = 30, 000 m^2/L, [Pt] = 4500 ppm.

Ψ_0 is found at the equilibrium (final) pH value using the site balance [pH shift model Eq. (A.22)] and the Gouy–Chapman description of the diffuse layer [pH shift model Eq. (A.11)].

It should be noted that the counterion (Cl^-) is not included in the ionic strength term. It was found that quantitative agreement of the model to the high surface loading (30,000 m^2/L) data was best achieved in this manner. Fig. A1 illustrates two adsorption curves for PTA with and without the Cl^- counterion, with the upper curve being the better simulation of data. A possible physical justification for this usage is that at the high ionic strengths involved at the highest surface loadings, and given the large radius of the doubly hydrated PTA complex, the electric double-layer thickness is less than the distance to the adsorption plane. This aspect is being studied further.

References

[1] W.A. Spieker, J.R. Regalbuto, Chem. Eng. Sci. 56 (2002) 3491.
[2] J.P. Brunelle, Pure Appl. Chem. 50 (1978) 1211.
[3] W. Stumm, Chemistry of the Solid-Water Interface, Wiley–Interscience, 1992.
[4] Cr. Contescu, M.I. Vass, Appl. Catal. 33 (1987) 259.
[5] M.S. Heise, J.A. Schwarz, J. Colloid Interface Sci. 107 (1985) 237.
[6] M.S. Heise, J.A. Schwarz, J. Colloid Interface Sci. 113 (1986) 55.
[7] M.S. Heise, J.A. Schwarz, J. Colloid Interface Sci. 123 (1988) 51.
[8] M.S. Heise, J.A. Schwarz, J. Colloid Interface Sci. 135 (1990) 461.
[9] H.A. Benesi, et al., J. Catal. 10 (1968) 328.
[10] R.D. Gonzalez, W. Zou, Catal. Lett. 15 (1992) 443.
[11] G.C. Bond, P.B. Wells, Appl. Catal. 18 (1985) 225.
[12] M. Arai, S.L. Guo, Y. Niahiyama, Appl. Catal. 77 (1991) 141.
[13] A. Goguet, J.P. Candy, et al., J. Catal. 209 (2002) 135.
[14] T.W. Healy, R.O. James, J. Colloid Interface Sci. 40 (1972) 65.
[15] J. Park, J.R. Regalbuto, J. Colloid Interface Sci. 175 (1995) 239.
[16] K.A. Agashe, J.R. Regalbuto, J. Colloid Interface Sci. 185 (1997) 174.
[17] X. Hao, J.R. Regalbuto, J. Colloid Interface Sci. 267 (2003) 259.
[18] J.R. Regalbuto, A. Navada, S. Shadid, M.L. Bricker, Q. Chen, J. Catal. 184 (1999) 335.
[19] M. Schreier, et al., manuscript in preparation.
[20] N. Santhanam, et al., Catal. Today 21 (1994) 141.
[21] R.O. James, G.A. Park, Surface Colloid Sci. 12 (1982) 119.
[22] J.S. Noh, J.A. Schwarz, J. Colloid Interface Sci. 139 (1989) 139.
[23] B.A. Morrow, A.J. McFarlan, Langmuir 7 (1991) 1695.
[24] W.A. Spieker, PhD dissertation, U. Illinois at Chicago (2001).
[25] P.A. Sermon, J. Sivalingam, Colloids Surf. 63 (1992) 59.
[26] J.T. Miller, M. Schreier, A.J. Kropf, J.R. Regalbuto, submitted for publication.